Hyperbolic secant slit lens for subwavelength focusing of light

A. G. Nalimov* and V. V. Kotlyar

Image Processing Systems Institute of the Russian Academy of Sciences, Molodogvardeyskaya st., 151, 443001 Samara, Russia
**Corresponding author: anton@smr.ru*

Received May 17, 2013; accepted June 17, 2013;
posted June 26, 2013 (Doc. ID 190726); published July 23, 2013

Using the finite-difference time-domain simulation, we show that if a gradient-index or binary planar dielectric microlens that focuses light at the output surface has a near-focus subwavelength slit the focal spot width is determined by the slit width. Notably, the slit allows the output light proportion to be increased due to the surface wave scattering, thus forming a focal spot nearly devoid of side lobes. In this work, the focal spot width of $\lambda/23$ and the diffraction efficiency of focusing of 44% are achieved. © 2013 Optical Society of America

OCIS codes: (130.3120) Integrated optics devices; (050.5298) Photonic crystals; (260.1960) Diffraction theory.
http://dx.doi.org/10.1364/OL.38.002702

The tight focusing of light near the interface surface has been performed with the aid of nanoslits [1,2]. In [1], a focal spot of size $\sim\lambda/2$ was generated using a "subwavelength generator" consisting of two 80 nm slits. Lenses with nanoscale slits made in gold were reported in [2] in which the incident light having passed through 20 nm slits was focused into a focal spot of about half-wavelength in width. In [3], light confinement in metamaterial was discussed, with the waves passing through two or more slits. Having passed through 20 nm slits in a screen, the light waves underwent diffraction in the metamaterial, forming a focal spot of the full width at half-maximum intensity FWHM $= \lambda/17$. However, the authors have failed to explain in which way, being so sharp, the focal spot could be output from the metamaterial. A nanoslit tens of nanometers wide can be used for confining and guiding light waves, similar to a waveguide [4]. The nanoslits have been used in this way in near-field microscopy [5]. The light scattered by the surface of the specimen under study passes through a slit in the cantilever and arrives to a high NA objective lens.

On the other hand, it is possible to perform the tight focusing of light using graded-index microlenses, in particular, planar photonic crystal lenses [5,6]. In [7], the focusing into a spot of size about $\lambda/4$ was performed with the aid of an array of holes in a taper. The diffraction of light from a nanoslit in metamaterial was analyzed in [8,9]. Obtaining of focal spots of size FWHM $= \lambda/10$ [8] and FWHM $= \lambda/5$ [9] was reported. The lens utilized in [8,9] contained dozens of 5 nm thick silver layers on top of 10 nm thick SiC. Note, however, that such a lens is difficult to realize in practice.

In this work, we combine the advantages of using a several-dozen nanometers wide slit for light confinement [4] and a gradient lens for the sharp focusing of light [10]. The finite-difference time-domain (FDTD) simulation has shown that a planar binary microlens in silicon with a 50 nm wide slit can generate a near-surface focal spot of size FWHM $= \lambda/23$ with a 44% energy efficiency. This value is smaller than those reported in the aforementioned works. With the focus occurring near the lens surface, it may find use in various nanophotonics applications. The nanoslit placed near the lens output surface in the focus region serves the dual function. The portion of TM-waves that propagate at small angles to the optical axis is confined by the nanoslit so that the nanoslit size defines the focal spot size. In the meantime, the portion of radiation that comes to the focus at larger-than-critical angles relative to the optical axis, generating a surface wave, are being scattered by the nanoslit and output from the lens, thus increasing the focusing efficiency.

Figure 1 depicts a scheme of a planar graded-index slit lens. We consider a hyperbolic secant (HS) lens whose refractive index depends on the transverse coordinate x as follows [10]: $n(x) = n_0 ch^{-1}[\pi x/(2H)]$, where n_0 is the refractive index on the axis and H is the lens length.

The slit in the planar HS lens of width W_1 is located on the optical axis, stretching as far as the lens output plane. The slit can be extended through the entire lens ($W_2 = H$) or found in the lens' rear section ($W_2 < H$). The light was propagated through the lens by the FDTD simulation implemented using the commercial software FullWave (by RSoft) and the software MEEP. The simulation parameters were as follows: the computation domain, 8 μm × 4 μm; incidence wavelength, 1.55 μm; and the computation domain step on the X and Y axes, $\lambda/500$. Figure 2 depicts the intensity distribution profile in the focal plane of a slitless ($W_1 = 0$) lens 10 nm after the lens output plane. The simulation parameters were $H = 1.95$ μm, $L = 4.8$ μm, the refractive index on the optical axis, $n_0 = 3.47$ (silicon), for a plane incident TE-wave. The lens length H was fitted to obtain the

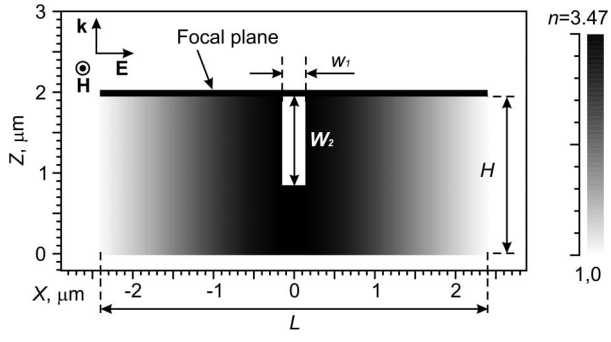

Fig. 1. (Gray-level) refractive index distribution of a HS slit lens: **k** is the wave vector, and **E** and **H** are the electric and magnetic field strength.

 © 2013 Optical Society of America

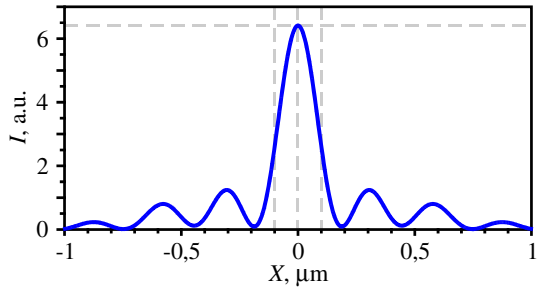

Fig. 2. Intensity profile in the focal plane $|E_y|^2$ generated by a slitless lens with the incident TE-wave.

minimal focal spot. For the TM-wave, the slitless graded-index lens would produce a four-times wider focal spot.

The focal spot in Fig. 2 has a size of FWHM $= 0.117\lambda$. This value is smaller than the diffraction-limited spot size for silicon: FWHM $= 0.44(\lambda/3.47) = 0.127\lambda$. The intensity peak in Fig. 2 is six times larger than the incident pulse intensity. We can show that using a slit on the lens optical axis with $n = 1$ and the incident TM-wave, it is possible to obtain a sharper focal spot. Figure 3(a) shows the focal spot width FWHM as a function of the slit width W_1. The slit length is assumed to be equal to the lens length: $W_2 = H = 2.2$ μm, the rest of the simulation parameters being the same as in Fig. 2. Note that the simulation results obtained using the FullWave software are in good agreement with a similar simulation of the lens performance conducted using the MEEP software.

From Fig. 3(a) the focal spot width FWHM is seen to be a linear function of the slit width W_1. The focal spot is slightly wider than the slit. Figure 3(b) shows the intensity profile in the lens focus at $W_1 = 50$ nm.

The light confinement in the nanoslit can be explained in a similar way to generating a fundamental TM-mode in a planar slitted waveguide [4]. In this case, the field within the slit is described by the relation

$$E_x(x,z) = \exp(i\beta x)ch[(\beta^2 - k^2)^{1/2}|x|], \qquad |x| < a,$$

where α is the nanoslit boundary coordinate, $2\alpha = W_1$, β is the propagation constant of the fundamental TM-mode, and k is the wavenumber in vacuum.

Figure 3(b) shows that there is an intensity dip in the focal spot center defined by a hyperbolic cosine. The field amplitude $E_x(x,z)$ undergoes a breakdown at the slit boundary $|x| = a$, so that near the slit at $|x| > a$ the amplitude is n^2 times decreased. Considering that Fig. 3(b) shows the intensity profile calculated at distance 10 nm after the lens, the focal spot intensity peak is wider if compared to that produced by the lens. Besides, the intensity peak in the focus center is smaller compared to that observed in the slit.

The diffraction efficiency (DE) of focusing η_D depends on the slit width W_1. The DE is maximal at $W_1 \approx 40$ nm. With increasing slit width, the DE η_D is decreasing [Fig. 4(a)] because the light intensity in the focus is decreasing with increasing W_1 [Fig. 4(b)]. The DE η_D was calculated as the ratio of the energy contained in the central lobe of the focal diffraction pattern (on the interval -75 nm $< x < 75$ nm) to the entire energy reaching the output plane of width L. It can also be seen from Fig. 3(a) that for $W_1 < 5$ nm the focal spot size starts to grow. The minimal focal spot size FWHM is achieved at $W_1 = 5$ nm, being equal to FWHM $= \lambda/119$ at distance 10 nm after the lens. For comparison, the focal spot in Fig. 2 has FWHM $= \lambda/8$ and the DE $\eta_D = 60\%$.

From Fig. 4 it is seen that the maximal DE is $\eta_D = 39.9\%$, whereas the focal spot size is FWHM $= \lambda/28$ [Fig. 3(a)]. In [4] it was demonstrated that in the silicon waveguide less than 30% of the waveguide mode optical energy was confined in nanoslits of an arbitrary size (ranging from 10 to 150 nm).

Figures 5(a) and 5(b) depict the DE η_D and the focal intensity I as a function of the slit length W_2, respectively, assuming the slit width $W_1 = 50$ nm. In calculating η_D, the focal spot size was again considered up to the nearest side-lobes, -75 nm $< x < 75$ nm. From Fig. 5 it is seen that the maximal values of the DE $\eta_D = 43.4\%$ and intensity I are observed when the slit length is chosen so as to provide a $\lambda/2$ phase delay, i.e., at $W_2 = \lambda[2(n_0 - 1)]^{-1} = 0.314$ μm. We note that the optical intensity in the lens focus is about 20% larger than for $W_2 = H$.

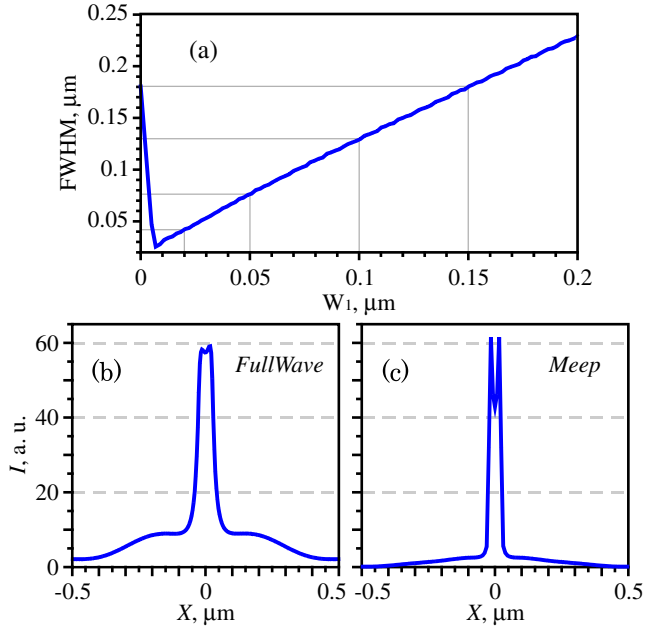

Fig. 3. (a) Focal spot width FWHM as a function of the slit width W_1 and the intensity profile $I = |E_x|^2 + |E_z|^2$ in the focal plane (10 nm after the lens) at $W_1 = 50$ nm, simulated using the (b) FullWave and (c) MEEP software.

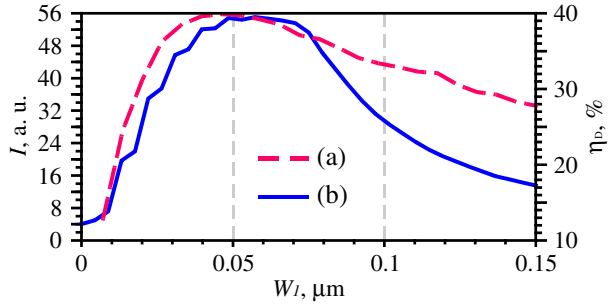

Fig. 4. (a) DE η_D and (b) intensity at the lens focus (10 nm apart from the lens) as a function of the slit width W_1, at $W_2 = H$.

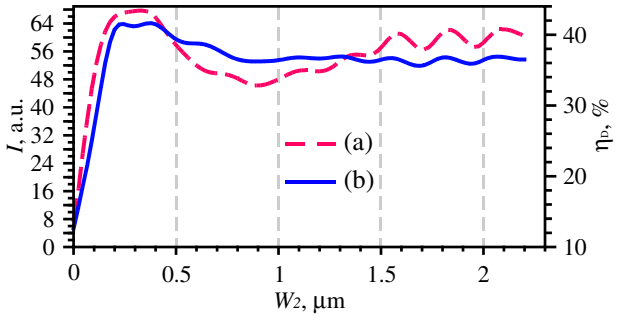

Fig. 5. (a) DE η_D and (b) intensity I in the lens focus as a function of the slit length W_2, at $W_1 = 50$ nm.

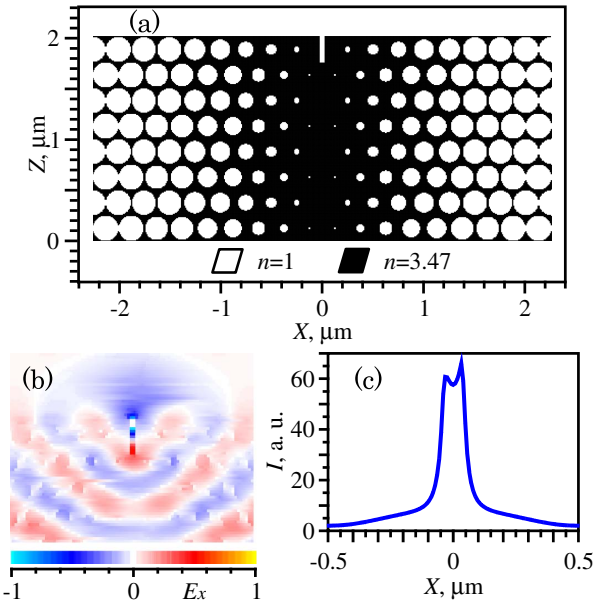

Fig. 6. (a) Refractive index distribution in a photonic crystal lens with a slit. (b) The instantaneous distribution of the field E_x in such a lens at instance $cT = 32$ μm. (c) Intensity profile in the transverse focal plane 10 nm after the lens.

Considering that the fabrication of a graded-index lens using the state-of-the-art nanolithography techniques presents a challenge, the described sharp focusing of the TM-wave can be implemented using a photonic crystal lens with a slit on the optical axis, which would be analogous to the graded-index lens in terms of the average refractive index distribution. Figure 6(a) depicts the refractive index distribution in the X–Z plane of a photonic crystal lens similar to the graded-index lens of Fig. 1.

The lens in Fig. 6(a) consists of 8 rows of holes on the Z axis and 20 rows of holes on the X axis arranged in a staggered order. The holes' centers are arranged with a period of 266 nm on the X axis and 250 nm on the Y axis. The minimal hole diameter is 30 nm, maximal is 250 nm, the lens length is 2 μm, width is 4.8 μm, the lens material refractive index is $n = 3.47$, $W_1 = 50$ nm, and $W_2 = 0.25$ μm. For such a lens, the value of η_D depends on the slit length W_2 at $W_1 = 50$ nm in a similar way to the graded-index lens, as seen from Fig. 6(b). The maximal DE is $\eta_D = 44.3\%$ at $W_2 = 250$ nm. In this case, the focal spot size is FWHM $= \lambda/23$, with the focal spot intensity being 60 times higher than the incident wave intensity. If such a lens is illuminated by a Gaussian beam with a waist radius of $\sigma = 2.4$ μm, the focal spot shape is preserved but the focal spot intensity is 1.7-times decreased.

Summing up, using the 2D FDTD simulation, we have shown that if a planar graded-index HS microlens of size 2 μm × 5 μm in silicon that contains on the optical axis a nanoslit of width 50 nm and length ~300 nm is illuminated by a plane TM-wave, a focal spot of width FWHM $= \lambda/28c$ is generated at the lens output with the DE $\eta_D = 43\%$.

The work was partially funded by the RF Ministry of Education and Science under Federal program "Research and Academic Cadres of Innovative Russia" (Agreement No. 8027), RF President's grants for Support of Leading Scientific Schools (NSh-4128.2012.9), a Young Candidate of Science grant (MK-3912.2012.2), and RFBR grants (12-07-00269, 12-07-31117, 13-07-97008).

References

1. K. R. Chen, Opt. Lett. **35**, 3763 (2010).
2. S. Ishii, A. V. Kildishev, V. M. Shalaev, K.-P. Chen, and V. P. Drachev, in *Conference on Lasers and Electro-Optics* (2011).
3. G. Ren, C. Wang, Z. Zhao, X. Tao, and X. Luo, J. Opt. Soc. Am. B **29**, 3103 (2012).
4. V. R. Almeida, Q. Xu, C. A. Barrios, and M. Lipson, Opt. Lett. **29**, 1209 (2004).
5. H. T. Chien and C. C. Chen, Opt. Express **14**, 10759 (2006).
6. H. Kurt and D. S. Citrin, Opt. Express **15**, 1240 (2007).
7. Z. Cheng, X. Chen, C. Y. Wong, K. Xu, C. K. Y. Fung, Y. M. Chen, and H. K. Tsang, Opt. Lett. **37**, 1217 (2012).
8. G. Ren, Z. Lai, C. Wang, Q. Feng, L. Liu, K. Liu, and X. Luo, Opt. Express **18**, 18151 (2010).
9. G. Li, J. Li, and K. W. Cheah, Appl. Opt. **50**, G27 (2011).
10. V. V. Kotlyar, A. A. Kovalev, A. G. Nalimov, and S. S. Stafeev, Adv. Opt. Technol. **2012**, 1 (2012).